

Non-destructive measurement of fuel rods inner pressure and composition: numerical consideration of different spring dimensions.

D. Ayache¹, S. Gillet², L. Ramiandrisoa³, C. Reece², JY. Ferrandis^{1,*}

¹IES, University of Montpellier, CNRS, Montpellier (France)

²DCN/PEL/DER, EDF, Saint-Denis (France)

³R&D/PRISME, EDF, Chatou (France)

(*) jean-yves.ferrandis@umontpellier.fr

Abstract—The technique presented in this paper enables non-destructive measurement of both the internal pressure and gas composition within fuel rods used in pressurised water reactors. The sensor consists of a piezoelectric element shaped as a tile, which can be applied directly on the fuel rod cladding in the plenum region, where fission gases accumulate. Acoustic waves generated by the sensor propagate inside the cladding and the reflections occurring within the gas are detected. The time-of-flight between measured echoes is used to retrieve the composition of the internal gas mixture. Pressure is related to the amplitude of the acoustic signal and is determined through a calibration process that links theoretical amplitude to experimental measurements. The developed theoretical model significantly reduces the calibration time by taking into account the losses and signal attenuation caused by the presence of a spring located within the measurement zone. This paper presents the construction of a theoretical model that considers the effects of the pressure and gas composition, as well as the shadowing and diffraction phenomena induced by the spring, all of which influence the amplitude of the measured acoustic signal.

Keywords — Acoustic, Non-Destructive Testing, Fuel rods, Pressurized Water Reactors.

I. INTRODUCTION

This work presents the development of an innovative, non-destructive acoustic technique for in situ measurement of internal pressure and gas composition within the upper plenum of standard pressurised-water reactor (PWR) fuel rods. The proposed technique is designed to be cost-effective, straightforward to implement and suitable for deployment directly at nuclear power plant (NPP) sites.

Internal rod pressure is one of many critical parameters of engineering and safety criteria, such as cladding corrosion, against which the acceptable burn-up limits for nuclear fuel are defined. Accurate pressure monitoring is essential to prevent localised swelling or mechanical degradation of the cladding. Additionally, internal pressure serves as a key indicator of the overall behaviour of the fuel rod during operation, transport and long-term storage and can offer insights into gas desorption dynamics.

A strong correlation exists between internal pressure and gas composition. The latter reflects the release of noble fission gases—primarily helium (He), krypton (Kr) and xenon (Xe)—into the rod's free volume [1], [2]. Acoustic techniques enable a direct inventory of these released gases, thus providing valuable information about the fuel performance and fission gas release behaviour.

Such data are also essential for code validation and multi-physics simulation tools used in nuclear engineering [3]. However, current methodologies in France require the extraction of fuel rods followed by their transport to specialised hot laboratories using dedicated casks. These operations are expensive, time-consuming and involve radiation risks. Once in the laboratory, the rods are pierced and cannot be used anymore, resulting in the generation of nuclear waste.

The development of a non-destructive, on-site measurement, would prevent the need for complex logistics and both operational costs and nuclear waste production. Furthermore, it would enable larger measurement campaigns across fuel assemblies, thus supporting the creation of statistically robust datasets and the development of probabilistic models. Finally, this technique could provide an alternative approach to the detection of leaking fuel rods, which is currently performed using ultrasonic inspection methods across the French nuclear fleet.

EDF, French energy supplier, and IES (University of Montpellier, CNRS) have collaborated for more than 20 years to develop a methodology for on-site measurements. The first generation of the developed system was successfully used on irradiated fuel rods in the LECA-STAR facility at the CEA CADARACHE Centre [4]. The latest improvements of the system have demonstrated the feasibility of the measurement for pressure below 40 bar in pure helium (100% He), covering a wider range of the fuel cycle.

The challenge of the measurement lies in the different parameters, which can evolve during the fuel cycle and need to be considered. The spring used to mechanically maintain the fuel pellets inside the rod constitutes one of the most important parameters to consider as it can significantly affect the pressure measurement. There are two different approaches to assess the effect of the spring. The first is to include it directly in the calibration process that links the theoretical model to the experiments. However, this requires having specific calibration

for each existing spring configuration. Given the variation of spring geometry between manufacturers and fuel assemblies, this would make the calibration process complex and time-consuming. The second approach is to describe the effect of the spring using explicit analytical equations within the theoretical model. This allows the calibration process to be decoupled from the different spring dimensions that can be encountered. The consideration, by the numerical model, of the different types of springs leading to the validation of the system in laboratory conditions will be presented in this paper.

II. PRESENTATION OF THE SYSTEM

The next section will provide a brief description of the acoustic sensor and the principle of the measurement. More detailed information can be found in [5-7].

A. Acoustic sensor design

The acoustic transducer has a tile shape designed as concentric to the fuel rod. Fig. 1 shows a representation of the device. The sensor is the complete system composed of different layers including a backing, a piezoelectric element and a coupling material with the rod cladding.

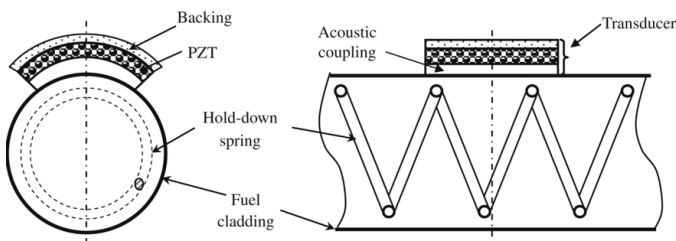


Fig. 1. Schematic representation of the acoustic device. Fuel rod inner diameter $D = 8.3$ mm and thickness $e = 0.57$ mm [5].

The design and the optimisation of the acoustic device layers are defined through the stacking model presented in [8] which enables the control of the thickness of the different layers, the electromechanical properties of the piezoelectric element and the acoustic velocity, the density and the attenuation of the layers.

The sensor can be operated in two frequency ranges: frequency 1 (f_1) around 3–4 MHz and frequency 2 (f_2) around 7–8 MHz, each representing different gas concentration ranges. For gas mixtures containing more than 5% Xe/He (i.e., 5% Xe and 95% He), the measurement is performed at f_1 . For mixtures containing less than 5% Xe/He, it is more efficient to work at f_2 . Indeed, since the speed of sound is higher in He, it is challenging to identify the first echoes in the measured signal at f_1 , as they tend to be lost in the background noise.

Several mounting configurations can be used depending on the application (Fig. 2):

- A “clamp”, used in testing and qualification phase in laboratory
- A “weight”, specifically designed for hot lab applications. It consists of two metallic masses tied to the sensor. This auto positioning system ensures good coupling between the sensor and the rod.
- A “saber”, with a miniaturized version of the sensor to perform, that can be mounted on a motorized arm to

perform measurements on peripheral but also fuel rods positioned inside the assembly.

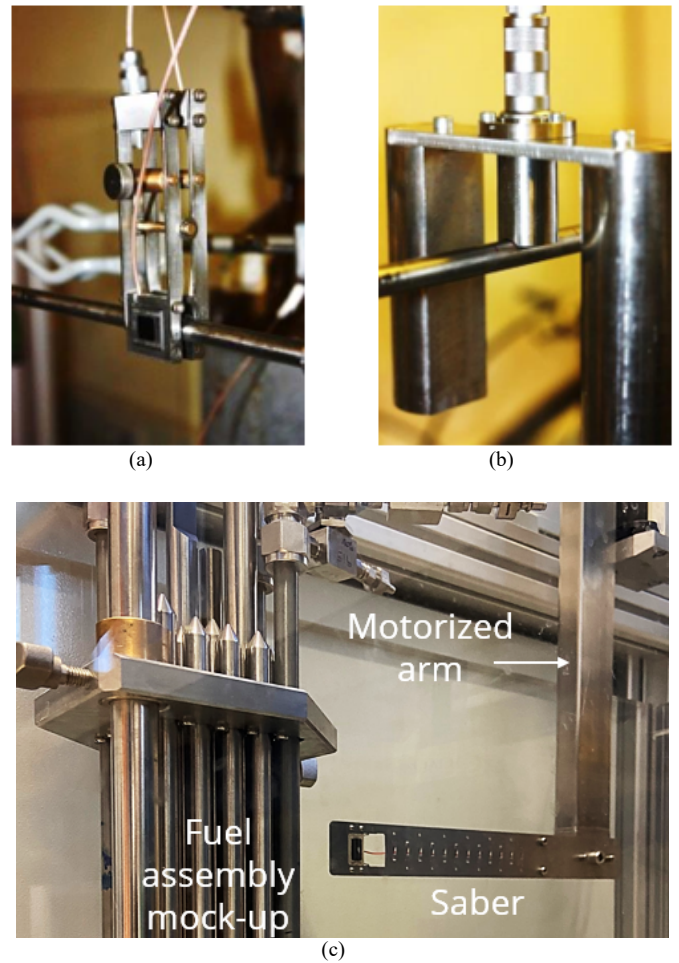


Fig. 2. Different types of mounting configurations for the sensor (a) “clamp”, (b) “weight” and (c) “saber”.

B. Principle of the measurement

Acoustic waves, generated by the piezoelectric transducer, propagate through the rod cladding and inside the gaseous mixture. Therefore, a modification in the frequency spectrum of the vibration of the gas can be observed. The acoustic impedance of a gas in a rigid plane cavity is described as a periodic function. The resonances of the gas are separated with a frequency Δf described in (1):

$$\Delta f = \frac{c_{gas}}{2D} \quad (1)$$

where c_{gas} is the sound velocity in $m \cdot s^{-1}$ and D is the inner diameter of the rod in m.

Then, the sound velocity can be computed from (1) to deduce the molar mass M of the gas mixture (2):

$$M = \frac{\gamma RT}{c_{gas}^2} = xM_{Xe} + (1-x)M_{He} \quad (2)$$

where x is the molar fraction of xenon in a gas mixture composed of helium and xenon, γ is the adiabatic index equal to $\frac{5}{3}$ for a monoatomic gas and T is the temperature in K.

In our application, the composition of the gaseous mixture involves a small amount of krypton. In order to retrieve its composition, the molar mass is described as in (3):

$$M = xM_{Xe} + \frac{x}{x_{Kr}}M_{Kr} + \left(1 - x - \frac{x}{x_{Kr}}\right)M_{He} \quad (3)$$

In (3), the ratio of the concentration of xenon to the concentration of krypton is known and assumed to be equal to 17 or 10 for UO₂ or MOX fuel. This assumption is true after the first fuel cycle and results from measurements carried out by the CEA on several fuel rods and is confirmed by previous studies [9].

The gas mixture composed of He-Xe-Kr is not a perfect gas, which implies that the sound velocity increases with the pressure. Therefore, as the pressure range during the tests varies from 0 to 80 bar, some corrections must be applied to the sound velocity as described in (4):

$$c_{gas}^2 = \frac{5RT}{3M} \left(1 + \left(2b - \frac{a}{RT^{\frac{3}{2}}}\right) \frac{P}{RM}\right) \quad (4)$$

where P is the pressure and the adjustable quantities a and b are obtained from [10].

In Fig. 3, an echogram, i.e., the reflection of the acoustic wave inside the medium, can be observed.

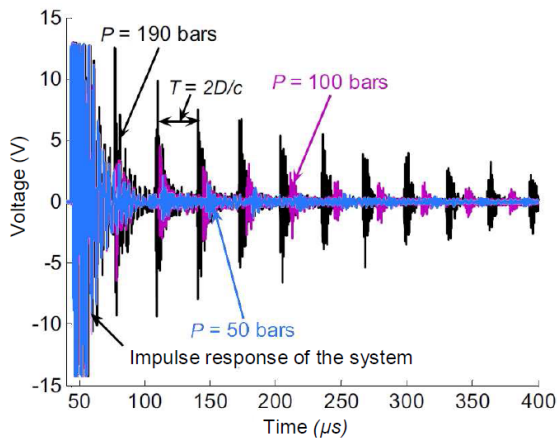


Fig. 3. Echogram obtained for a gas mixture of 40 % of argon (Ar) in He and for pressure equal to 50 bar, 100 bar and 190 bar [11].

The echograms presented in Fig. 3 characterize a gas mixture of 40 % Ar/He. The period between two echoes, usually called the time-of-flight (ToF), is used to calculate the sound velocity and retrieve the gas composition as previously explained. Moreover, it can be observed that the amplitude of the different echoes increases with the pressure, which makes it possible to determine the pressure through a calibration process.

The pressure is not the only parameter affecting the amplitude of the measured signal. In the next section, the effect of the gas composition and the presence of the spring in the plenum part on the measured amplitude will be described.

III. PARAMETERS AFFECTING THE SIGNAL AMPLITUDE

The theoretical amplitude Amp_{th} of the signal is defined as in (5):

$$Amp_{th} = P \times \sqrt{M} \times Absorption^{je} \times Losses^{je} \quad (5)$$

where P is the pressure in bar, M is the molar mass of the gas in g.mol⁻¹, $Absorption$ represents the losses induced by the gas as an absorption medium and $Losses$ defines the losses induced by the presence of a spring. The losses in the system depend on the echo order je .

A. Effect of the pressure

The effect of the pressure on the signal amplitude can be observed in Fig. 4. The echograms are obtained in pure helium for 3 different pressures: 80 bar, 40 bar and 30 bar. In Fig. 4 the envelope of each echo is obtained after signal processing including double FFTs, signal filtering at f_1 or f_2 and correlation with theoretical echoes implemented to increase the noise rejection. In this case, the measurement is performed at $f_2 = 7.95$ MHz. The experimental setup is detailed in part IV.

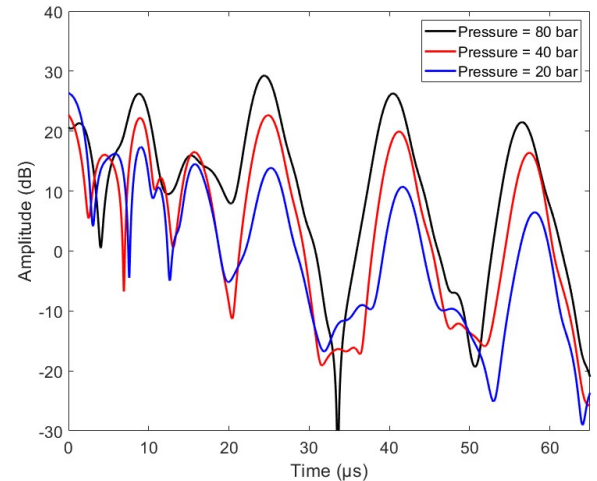


Fig. 4. Effect of the pressure on the amplitude of the signal. Echograms obtained for 100% He at different pressures: 80 bar (black curve), 40 bar (red curve) and 20 bar (blue curve). Measurements performed at ambient room temperature (20.5 °C) and the sensor operated at $f_2 = 7.95$ MHz.

The sound velocity is higher in pure He which complicates the separation of the first echo from the noise. For the second echo of the signal observed at 25 μ s, the amplitude of the signal decreases from about 30 dB at 80 bar to 13 dB at 20 bar. This shows that for a stable composition, the amplitude of the measured signal decreases when the pressure decreases.

B. Effect of the gas composition

Fig. 5. shows the effect of the gas composition and the absorption induced by the gas. The echograms are obtained at 70 bar in two different gas mixtures: 20% Xe/He and 10% Xe/He. In this case the sensor is operated at $f_1 = 3.68$ MHz. The gas composition has an effect on the period and the amplitude of the signal that varies even for a stable pressure.

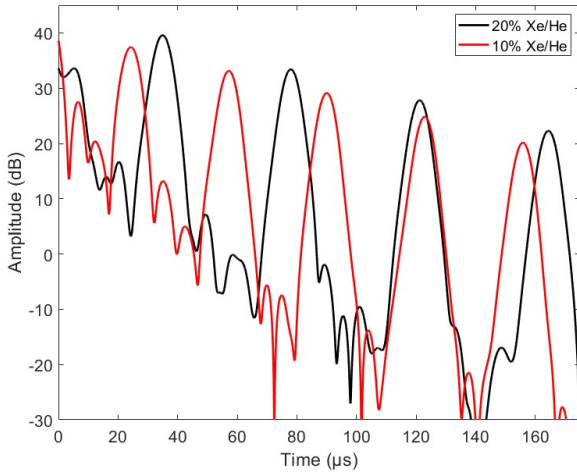


Fig. 5. Effect of the gas composition on the amplitude of the signal. Echograms obtained at 70 bar for different gas mixtures: 20% Xe/He (black curve), 10% Xe/He (red curve). Measurements performed at ambient room temperature (20 °C) and the sensor operated at $f_1 = 3.68$ MHz.

C. Effect of the spring

The echograms are obtained in pure He at 70 bar with $f_2 = 7.95$ MHz. In Fig. 6, three different configurations are presented: without a spring, with a spring type A and a spring type B. The pitch g of the spring is about 7.8 mm and 4.5 mm and the wire diameter d is equal to 1.2 mm and 1.5 mm, respectively, for spring A and spring B.

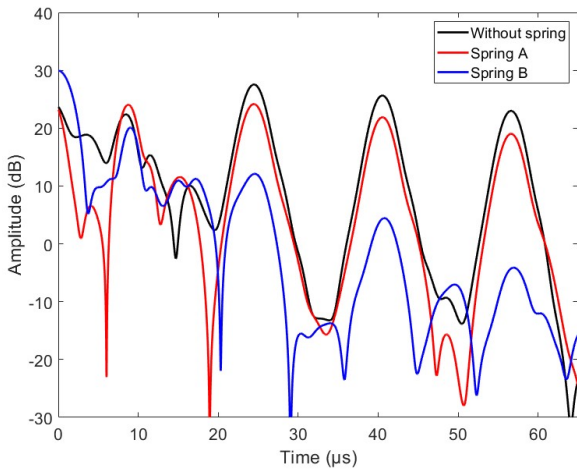


Fig. 6. Effect of the presence of a spring in the measurement zone on the amplitude of the signal. Echograms obtained at 70 bar in pure He in three configurations: without spring (black curve), with spring A (pitch $g = 7.8$ mm, wire diameter $d = 1.2$ mm) (red curve) and spring B (pitch $g = 4.5$ mm, wire diameter $d = 1.5$ mm) (blue curve). Measurements performed at ambient room temperature (20.5 °C) and the sensor operated at $f_2 = 7.95$ MHz.

In Fig. 6, it can be observed that for the same experimental condition of pressure and composition, the amplitude of the signal decreases with the presence of the spring. Moreover, spring A is less compressed than spring B. The difference observed between the measurements performed on two different types of springs shows that the effect of the springs on the signal amplitude depends on their geometrical parameters.

If the experimental amplitude Amp_{exp} is defined as in (6) :

$$Amp_{exp} = S \times Amp_{th} \quad (6)$$

where S is a constant, then the losses, defined in (5), can either be a constant for each configuration of spring or defined by explicit equations taking into account the geometry of each spring. In the latter case, S would be a constant exclusively related to the type of sensor employed for the measurement.

1) Shadow effect

Part of the acoustic waves that are transmitted through the rod cladding will not propagate inside the gas due to the presence of the spring. In this case, the spring acts as a screen, blocking the propagation of the emitted signal and resulting in a reduction of the intensity of the waves. This phenomenon does not depend on the order of the echo je , and can be described as function of the geometrical parameter of the spring:

$$Shadow = 1 - \frac{2d}{g} \quad (7)$$

2) Diffraction effect

Diffraction occurs when the acoustic waves propagating inside the rod hit the surface of the spring. This phenomenon is function of the wavelength λ , thus the frequency, and the geometrical parameters of the spring:

$$Diff = \frac{1}{1 + \left(\frac{\lambda}{cste \times \left(\frac{g}{2} - d \right)} \right)^3 + \left(\frac{\lambda}{cste \times l} \right)^3} \quad (8)$$

where $cste$ is a constant equal to 190 obtained through empirical work and l is the width of the acoustic device approximately 10 mm.

D. Calibration and measurement processes

By injecting (7) and (8) in (6), the Amp_{exp} is defined as:

$$Amp_{exp} = S \times P \times \sqrt{M} \times Shadow \times (Absorption \times Diff)^{je} \quad (9)$$

During the calibration process, the pressure P , the gas composition, related to M and the spring dimension is known. Thus, the model can be used to calculate the theoretical amplitude of the signal. It is then possible to determine the constant S , by adjusting experimental and theoretical values for a few known values of pressure and composition.

During the measurements, S is known and related to the sensor properties. By inserting the spring dimensions in the theoretical model, the losses can be calculated and the pressure and gas composition retrieved.

IV. EXPERIMENTAL MEASUREMENT

The experimental setup is composed of a SEPEMA generator developed by SONAXIS company. This equipment is used as a pulse generator and a signal receptor and is capable of

performing data acquisition and processing. A single pulse of few nanoseconds targeting f_1 frequency range is sent to the sensor. The complete echogram is collected and signal processing is performed at f_1 and f_2 .

A homemade gas mixing system using calibrated gas bottles is used to fill the rod-mock available in our laboratory. A manometer is used to control and adjust the pressure inside the rod. The sensor is clamped over a rod with water as a coupling medium. The rod mock-up is long enough to contain two different types of spring: spring A, previously described, and spring C (pitch $g = 5.9$ mm and wire diameter $d = 1.5$ mm).

During the calibration process, measurements are performed at two different compositions and, in each case, for two different pressures. Therefore, the first measurements are conducted at 20% Xe/He for 70 bar and 50 bar. The second part of the process is conducted in pure helium for 70 bar and 50 bar. For each configuration of composition/pressure, the measurement is performed 3 times, where each represents the mean of 10 measurements performed at 10 different sensor positions. The calibration process is conducted on the zone containing the spring C, and the sensitivity S of the sensor is retrieved.

Measurements are then conducted on spring A and spring C. The rod is pressured at 30 bar, 40 bar, 50 bar and 70 bar with 20% Xe/He, 10% Xe/He and pure He. The pressure calculated by the model is compared to the reference pressure measured by the manometer with an acceptance interval of 15% defined by our industrial partner (Fig. 7). Signal processing is performed at $f_1 = 3.68$ MHz for measurement in 20% and 10% Xe/He and at $f_2 = 7.95$ MHz for pure He.

V. CONCLUSION

A non-destructive ultrasound-based technique for measuring the internal pressure and composition of PWR fuel rods has been developed. This work is part of a long-term collaboration between EDF and IES. The pressure is related to the amplitude of the acoustic signal. A theoretical model considering the effects of the pressure, gas composition and the presence of a spring in the measurement zone has been developed. This model is based on explicit equations describing the losses obtained through empirical work. The calibration process is now less time-consuming and exclusively related to the sensor, rather than varying spring configurations. This model has been successfully used to calculate the pressure from measurements obtained with different spring dimensions, achieving a success rate of 90%.

ACKNOWLEDGEMENTS

The authors would like to warmly thank G. Lévêque, former professor at IES, who mainly developed the theoretical aspects of the model presented in this paper.

They would also like to thank SONAXIS for manufacturing and supplying the sensors.

REFERENCES

- [1] D.R. Olander, Fundamental Aspects of Nuclear Fuel Elements, TID-26711-P1, US Department of Energy, 1976 (Chapter 15).
- [2] J. Siefken, SCRAP/RELAP5/MOD3.3 Code Manual, NUREG/CR-6150, vol.2, Rev. 2, INEL-96/0422, 2001.
- [3] D. Baron, P. Thevenin, R. Largenton, R. Masson, S. Pujet, R. Arnaud, Cyrano 3 the EDF fuel performance code especially designed for engineering applications, in: Water Reactor Fuel Performance Meeting Proceeding, Seoul, 2008.
- [4] J.Y. Ferrandis, E. Rosenkrantz, G. Leveque, D. Baron, J.C. Segura, G. Cecilia, O. Provitina, Full-scale Hot Cell Test of an Acoustic Sensor Dedicated to Measurement of the Internal Gas Pressure and Composition of a LWR Nuclear Fuel Rod, IEEE Transactions on Nuclear Science, 60(4), 2894-2897, 2013, <https://doi.org/10.1109/TNS.2013.2264111>
- [5] G. Leveque, E. Rosenkrantz and D. Baron, "Acoustic Injection into a Pressurized Gas Through a Metallic Wall", Acta Acustica united with Acustica, vol. 93, pp. 722-729, 2007.
- [6] E. Rosenkrantz, J.Y. Ferrandis, G. Leveque, D. Baron, "Ultrasonic measurement of gas pressure and composition for nuclear fuel rods", Nuclear Instruments and Methods in Physics Research Section A: Accelerators, Spectrometers, Detectors and Associated Equipment, Volume 603, Issue 3, 21 May 2009, Pages 504-509, <https://doi.org/10.1016/j.nima.2009.02.028>
- [7] E. Rosenkrantz, J.Y. Ferrandis, G. Leveque, D. Baron and P. Thevenin, "Ultrasonic method for nuclear fuel rods pressure and gas composition released measurement," 2009 1st International Conference on Advancements in Nuclear Instrumentation, Measurement Methods and their Applications, Marseille, France, 2009, pp. 1-5 <https://doi.org/10.1109/ANIMMA.2009.5503773>
- [8] "Caractérisation d'un gaz confiné à l'aide d'un capteur acoustique - Application aux crayons combustibles nucléaires", Ref. in 113, 2010 (in French), <https://doi.org/10.51257/a-v1-in113>
- [9] R. J. White, S. B. Fisher, P. M. A. Cook, R. Stratton, C. T. Walker, and I. D. Palmer, "Measurement and analysis of fission gas release from BNFL's SBR MOX fuel," Journal of Nuclear Materials, vol. 288, no. 1, pp. 43-56 (2001).
- [10] J.J. Hurly, J.W. Schmidt, S.J. Boyes, and M.R. Moldover, "Virial equation of state of helium, xenon, and helium-xenon mixtures from speed-of-sound and Burnett PpT measurements," International Journal of Thermophysics, vol. 18, no. 3, pp. 579, 579-634 (1997).
- [11] P. Vasseur, J.M. Barthoulot, G. Leveque and J.Y. Ferrandis, (2016). *Acoustic sensors devoted to the detection of leaking irradiated fuel rod in spent fuel pool*. American Nuclear Society-ANS, 555 North Kensington Avenue, La Grange Park, IL 60526 (United States).

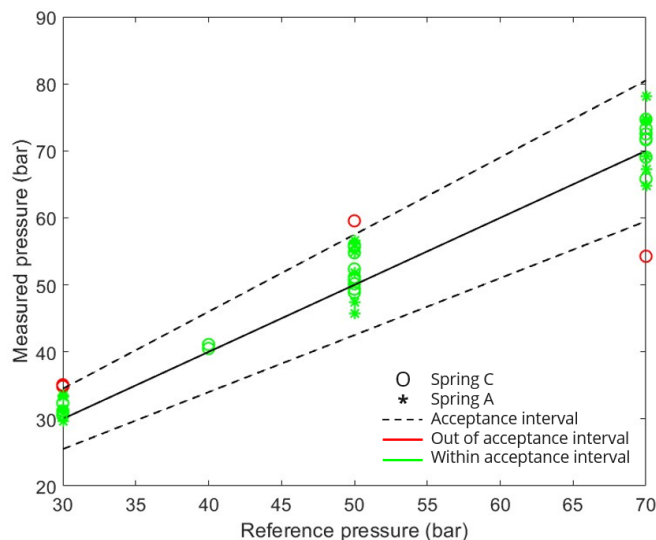


Fig. 7. Comparison of pressure calculated by the model with reference pressure measured by the manometer (black line) with an acceptance interval of $\pm 15\%$ (dashed line). Measurements are performed at ambient room temperature (20 °C). Measurements are conducted in two zones containing spring A (O) and spring C (*). Calculated pressures lying out of the acceptance interval are red and calculated pressures within the acceptance interval are green.

Fig. 7 shows 50 measurements conducted in different gas mixtures and at different pressures covering a large range values of the fuel cycle. For an acceptance interval of $\pm 15\%$ over the reference pressure, the model is capable of calculating pressures with a success ratio of 90%.